Independent optical excitation of distinct neural populations

Nathan C Klapoetke[1–5], Yasunobu Murata[4,5], Sung Soo Kim[6], Stefan R Pulver[6], Amanda Birdsey-Benson[4,5], Yong Ku Cho[1–5], Tania K Morimoto[1–5], Amy S Chuong[1–5], Eric J Carpenter[7], Zhijian Tian[8], Jun Wang[8], Yinlong Xie[8], Zhixiang Yan[8], Yong Zhang[8], Brian Y Chow[9], Barbara Surek[10], Michael Melkonian[10], Vivek Jayaraman[6], Martha Constantine-Paton[4,5], Gane Ka-Shu Wong[7,8,11] & Edward S Boyden[1–5]

Optogenetic tools enable examination of how specific cell types contribute to brain circuit functions. A long-standing question is whether it is possible to independently activate two distinct neural populations in mammalian brain tissue. Such a capability would enable the study of how different synapses or pathways interact to encode information in the brain. Here we describe two channelrhodopsins, Chronos and Chrimson, discovered through sequencing and physiological characterization of opsins from over 100 species of alga. Chrimson's excitation spectrum is red shifted by 45 nm relative to previous channelrhodopsins and can enable experiments in which red light is preferred. We show minimal visual system–mediated behavioral interference when using Chrimson in neurobehavioral studies in *Drosophila melanogaster*. Chronos has faster kinetics than previous channelrhodopsins yet is effectively more light sensitive. Together these two reagents enable two-color activation of neural spiking and downstream synaptic transmission in independent neural populations without detectable cross-talk in mouse brain slice.

Microbial opsins, which are light-driven ion pumps and light-gated ion channels that can be genetically expressed in excitable cells, enable the optical activation or inhibition of the electrical activity of defined neuron types, axonal pathways or brain regions with millisecond resolution[1–6]. There exists an unmet need to independently drive pairs of light-driven ion channels with different colors of light, which would enable the independent activation of different cell populations. Many groups have used channelrhodopsins with peak wavelength sensitivity to green light in conjunction with channelrhodopsins with peak wavelength sensitivity to blue light to achieve differential spiking with yellow light[7–10], but residual neural spiking cross-talk in response to blue light stimulation remains due to the intrinsic blue absorption by the retinal chromophore[11,12]. This fundamental limitation means it is currently not possible to achieve robust, temporally precise independent two-color spiking using a red-shifted channelrhodopsin alongside channelrhodopsin-2 (ChR2) in mammalian brain tissue. Previous efforts to further red-shift opsins and reduce blue light sensitivity through mutagenesis have empirically proven difficult, with spectra remaining little red shifted beyond that of the first reported green-peaked channelrhodopsin, VChR1 (refs. 9,13,14). Similarly, efforts to further increase the blue light sensitivity of ChR2 have resulted in much slower channelrhodopsins[15–17], which elicit low-temporal-precision spiking in response to light pulses of up to 1 s or longer.

One potential strategy for achieving independent two-color excitation is engineering differences in blue light sensitivity between blue and red light–drivable channelrhodopsins. Then a low blue irradiance could drive precisely timed spikes with the blue light–drivable channelrhodopsin while eliciting only subthreshold depolarizations (not causing synaptic release) in neurons expressing the red light–drivable channelrhodopsin. To achieve these goals, we turned to the natural world, performing *de novo* transcriptome sequencing of 127 species of alga.

Chronos is a new blue and green light–drivable channelrhodopsin with kinetics faster than those of previous channelrhodopsins as well as high light sensitivity. Chrimson is a new red light–drivable channelrhodopsin with spectra that are red shifted 45 nm more than those of previous channelrhodopsins. Together, Chronos and Chrimson allow independent two-color spike driving of, and synaptic release from, distinct neural populations in mouse brain slice. In addition, Chronos represents an excellent general-use channelrhodopsin. Chrimson may enable temporally precise experiments requiring red light, such as deep tissue

[1]The MIT Media Laboratory, Synthetic Neurobiology Group, Massachusetts Institute of Technology (MIT), Cambridge, Massachusetts, USA. [2]Department of Biological Engineering, MIT, Cambridge, Massachusetts, USA. [3]MIT Center for Neurobiological Engineering, MIT, Cambridge, Massachusetts, USA. [4]Department of Brain and Cognitive Sciences, MIT, Cambridge, Massachusetts, USA. [5]MIT McGovern Institute for Brain Research, MIT, Cambridge, Massachusetts, USA. [6]Janelia Farm Research Campus, Howard Hughes Medical Institute, Ashburn, Virginia, USA. [7]Department of Biological Sciences, University of Alberta, Edmonton, Alberta, Canada. [8]Beijing Genomics Institute-Shenzhen, Shenzhen, China. [9]Department of Bioengineering, University of Pennsylvania, Philadelphia, Pennsylvania, USA. [10]Institute of Botany, Cologne Biocenter, University of Cologne, Cologne, Germany. [11]Department of Medicine, University of Alberta, Edmonton, Alberta, Canada. Correspondence should be addressed to E.S.B. (esb@media.mit.edu) or G.K.-S.W. (gane@ualberta.ca).

RECEIVED 23 SEPTEMBER 2013; ACCEPTED 10 JANUARY 2014; PUBLISHED ONLINE 9 FEBRUARY 2014; DOI:10.1038/NMETH.2836

targeting, or scenarios in which blue light is visually distracting. To the latter end, we demonstrate brain stimulation through the cuticle of *Drosophila* and reduction in visual system–triggered responses during optogenetic experiments. These tools may also serve as protein backbones for building future optogenetic tools with novel capabilities.

RESULTS

Discovering novel channelrhodopsins via *de novo* sequencing

In recent years, a number of channelrhodopsins have been engineered for neuroscientific applications[18], derived from four channelrhodopsin genes from *Chlamydomonas reinhardtii* or *Volvox carteri*. However, all known natural channelrhodopsins have blue-green (430- to 550-nm) spectral peaks[13,14,18,19], and engineered red-shifted channelrhodopsins such as C1V1 (ref. 9) and ReaChR[14] have peak wavelength sensitivity to green light (~545 nm) and a similar spectrum to VChR1 (ref. 7). Furthermore, existing channelrhodopsins exhibit an inverse relationship between two desired properties: high light sensitivity and fast kinetics[18]. We therefore sought to overcome these limitations by exploring the genetic diversity of natural channelrhodopsins.

We *de novo*–sequenced 127 algal transcriptomes[20] and identified 61 channelrhodopsin homologs, which we subsequently synthesized and screened for photocurrents in HEK293 cells via whole-cell patch clamp (**Supplementary Figs. 1–4** and **Supplementary Table 1**). Of these, we selected opsins with novel characteristics for further characterization in cultured neurons (**Fig. 1** and **Supplementary Table 2**), focusing primarily on photocurrent, wavelength sensitivity, kinetics and trafficking (**Fig. 1** and **Supplementary Figs. 5–9**). To avoid selection bias, we cotransfected all opsins into neurons with a secondary tdTomato plasmid, and we selected cells solely according to the presence of cytosolic tdTomato expression (**Supplementary Fig. 5a**,**b**). This unbiased selection method was applied throughout the paper in all culture experiments unless otherwise indicated.

We assessed wavelength sensitivity and photocurrent amplitude, using ChR2 for blue (470 nm) comparison and $C1V1_{TT}$ (ref. 9) for green (530 nm) and far-red (660 nm) comparison (**Fig. 1a–d**). Of the 20 opsins screened in neurons, we found 4 previously unknown channelrhodopsins, one each from the species *Chloromonas oogama* (CoChR), *Chloromonas subdivisa* (CsChR), *Stigeoclonium helveticum* (ShChR) and *Scherffelia dubia* (SdChR) that bore either significantly higher blue photocurrents than ChR2 ($P < 0.001$; ANOVA with Dunnett's *post hoc* test used for all multiway comparisons; **Fig. 1c**) or significantly higher green photocurrents than $C1V1_{TT}$ ($P < 0.001$; **Fig. 1b**). Additionally, we discovered the first reported yellow-peaked channelrhodopsin, CnChR1 from the species *Chlamydomonas noctigama*. CnChR1 had 660-nm far-red light photocurrents of 674 ± 120 pA ($n = 11$ cells; values throughout are mean ± s.e.m.), which are significantly higher (~30×, $P < 0.0001$; **Fig. 1a**,**d**) than those of $C1V1_{TT}$. Owing to its spectral sensitivity, we nicknamed this molecule 'Chrimson'. With a spectral peak at 590 nm, Chrimson is 45 nm more red shifted than previously known channelrhodopsins (**Fig. 1e** and **Supplementary Figs. 5d**,**e** and **9**).

Kinetic parameters and spiking performance

The ability to optically evoke spikes necessitates that channelrhodopsins possess not only photocurrents sufficient to depolarize the neuron cell membrane above its spike threshold, but also on-, off- and recovery kinetics fast enough to precisely control spike timing and fidelity[18,21]. Previously published green and red light–drivable channelrhodopsins have relatively slow off-kinetics, which limits their utility for high-frequency neural activation[14,18]. We characterized the kinetic properties of opsins with green photocurrents comparable to or higher than those of $C1V1_{TT}$ and found that only CsChR and ShChR had faster turn-on, turn-off and recovery kinetics (**Fig. 1f–h**). With a turn-on of 2.3 ± 0.3 ms ($n = 8$ cells) and a turn-off of 3.6 ± 0.2 ms ($n = 7$ cells), the *S. helveticum* channelrhodopsin ShChR possesses the fastest reported kinetics to date (**Supplementary Fig. 3**): we therefore nicknamed this molecule 'Chronos'.

We assessed Chronos's green light (530-nm) spiking fidelities at various irradiances and frequencies in cultured neurons (**Fig. 2a–c** and **Supplementary Figs. 10** and **11**). As expected from its fast kinetic properties, Chronos-mediated optical spiking replicated electrically driven spiking between 5 and 60 Hz (**Supplementary Fig. 11**). In contrast, CsChR reliably drove spikes only up to 20 Hz, and $C1V1_{TT}$ could not reliably drive spikes above 10 Hz even at the highest expression level (**Supplementary Figs. 10** and **11**). It has previously been noted that slow off-kinetics or poor recovery kinetics of channelrhodopsins can cause depolarization block or reduce photocurrents over sustained pulse trains[18]. Consistent with this observation, the spike failures we observed at high frequencies for CsChR and $C1V1_{TT}$ primarily occurred later in the pulse train (**Supplementary Fig. 10e**).

We next examined red light (625-nm)-evoked spiking fidelities. Consistent with the earlier photocurrent screening, Chrimson was the only opsin screened capable of red light–driven spiking with 5-ms pulses (**Fig. 2d**): these irradiances and pulse widths resulted in Chronos depolarizations of less than 1.5 mV (**Supplementary Fig. 12g**). However, Chrimson's slow kinetics of current decay after the cessation of light, or τ_{off}, of 21.4 ± 1.1 ms ($n = 11$ cells), in conjunction with its poor recovery kinetics, caused depolarization block and channelrhodopsin inactivation at frequencies exceeding 10 Hz (**Fig. 2e** and **Supplementary Fig. 12a–d**). We therefore optimized these parameters via mutagenesis, and we identified the K176R mutant, denoted as ChrimsonR, which sped up the off-kinetics to 15.8 ± 0.4 ms ($n = 5$ cells) without altering the red-shifted action spectrum (**Fig. 2f** and **Supplementary Fig. 12e**,**f**). This kinetics improvement enabled fast, reliable red light–driven spiking at frequencies of at least 20 Hz in both cultured neurons and acute cortical slice (**Fig. 2e** and **Supplementary Fig. 13**), comparable to the blue light spiking performance of the commonly used ChR2(H134R)[18,22]. We additionally found ChrimsonR to be capable of reliably eliciting spikes in cortical slice using >20-ms pulses of far-red light (735 nm) (**Supplementary Fig. 13**), which may be useful for *in vivo* scenarios in which deep-tissue light penetration, or lack of visual drive, is desired by the experimenter.

Use of Chrimson in *Drosophila*

Although optogenetic tools have become widely used in mammalian behavioral experiments, such tools have found more limited use in *Drosophila* experiments[23–27], possibly owing to strong innate behavioral artifacts induced by stimulation light reaching photosensitive regions[28] and poor cuticle penetration of blue light[29]. Optogenetics has therefore typically been used (i) in constrained circumstances in which light is delivered to

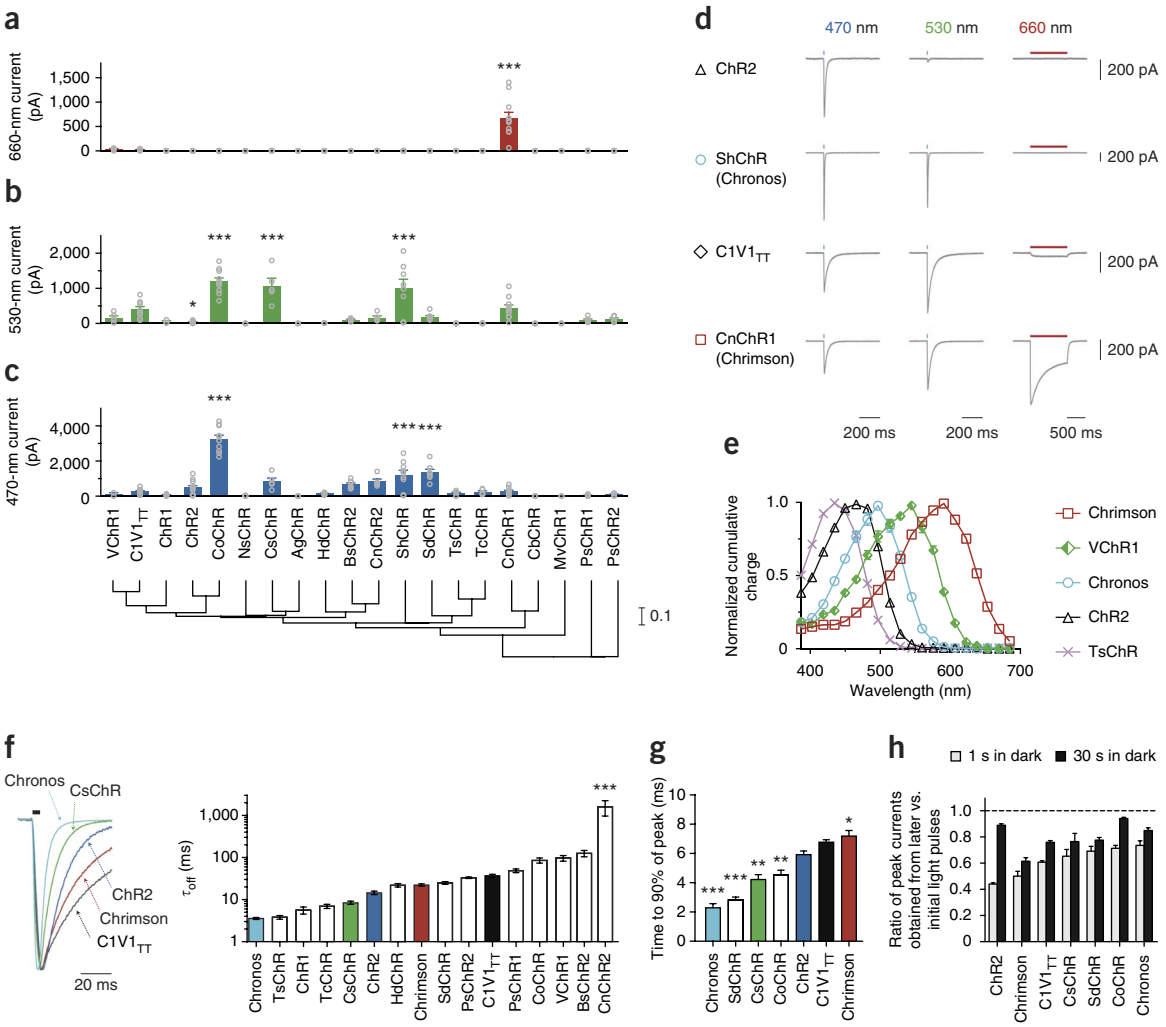

Figure 1 | Novel channelrhodopsin spectral classes discovered through algal transcriptome sequencing. (**a**–**c**) Maximum photocurrents in cultured neurons transfected with the different opsin-GFP fusions in response to far-red (660-nm), green (530-nm) and blue (470-nm) light; blue and green photon fluxes were matched, with illumination conditions defined as follows: 1-s pulse at 10 mW/mm^2 for red, 5-ms pulse at 3.66 mW/mm^2 for green and 5-ms pulse at 4.23 mW/mm^2 for blue. Individual cell photocurrents are plotted as gray circles and overlaid on the population bar graph. See **Supplementary Figure 6** for additional individual cell data. Bottom, phylogeny tree of the channelrhodopsins tested, based on transmembrane helix alignments. The scale indicates the number of substitutions per site. (**d**) Representative voltage-clamp traces in cultured neurons as measured under the screening conditions in **a**–**c** (the long red light pulse was used to ensure we did not miss any red-sensitive channelrhodopsins in our screen). (**e**) Channelrhodopsin action spectra (HEK293 cells; n = 6–8 cells; measured using equal photon fluxes, ~2.5 × 10^{21} photons/s/m^2). (**f**–**h**) Channelrhodopsin kinetic properties as measured in cultured neurons (see also **Supplementary Figs. 7** and **8**). Off-kinetics (**f**) were measured under the conditions in **a**–**c**; on-kinetics (**g**) and recovery kinetics (**h**) were measured with a 1-s pulse at 5 mW/mm^2. All opsins were illuminated near their respective peak wavelength, which was either blue or green for all opsins except Chrimson, which was characterized at 625 nm (n = 5–12 cells for all kinetic comparisons). τ_{off}, monoexponential fit of photocurrent decay. Peak current recovery ratios in **h** were determined from three 1-s light pulses, with the first pulse response used as the baseline for peak current recovery ratio calculations for both the second (1 s in dark after first pulse) and third pulse response (30 s in dark after second pulse). *P < 0.05, **P < 0.01, ***P < 0.001; ANOVA with Dunnett's *post hoc* test, with ChR2 as the reference in **c**,**f**,**g**, and C1V1$_{TT}$ as the reference in **a**,**b**. Exact P values and n values are in **Supplementary Table 2**. Plotted data are mean ± s.e.m. Opsins and the species they derive from are defined in the Online Methods.

peripheral organs while being blocked from reaching the eyes[25], (ii) in blind flies[23] or (iii) for cases in which undesired side effects of visible light stimulation do not substantially affect experimental interpretation[30]. Other technologies such as thermogenetics are often used despite their much slower time course[31,32]. We conjectured that red light activation with Chrimson, which is ~45 nm more red shifted than ReaChR[14,29] (**Supplementary Fig. 9**), would extend the reach of optogenetic tools to *Drosophila* behavioral experiments with reduced light-induced behavioral artifact and improved cuticle penetration.

We first used the *Drosophila* larval neuromuscular junction (NMJ) to examine the reliability of light-triggered action potentials in fly axons expressing Chrimson. Larval muscles have passive membrane properties, so excitatory junction potentials (EJPs) at the larval NMJ accurately reflect spiking in motor axons[31]. In Chrimson-expressing larvae, both 470-nm and 617-nm light triggered EJPs, even at short (1- to 2-ms) light-pulse durations and low intensities (0.06–0.14 mW/mm^2). In response to light-pulse durations over 2 ms, Chrimson activation triggered long-lasting barrages of EJPs (**Fig. 3a**,**b**). Long-wavelength red light

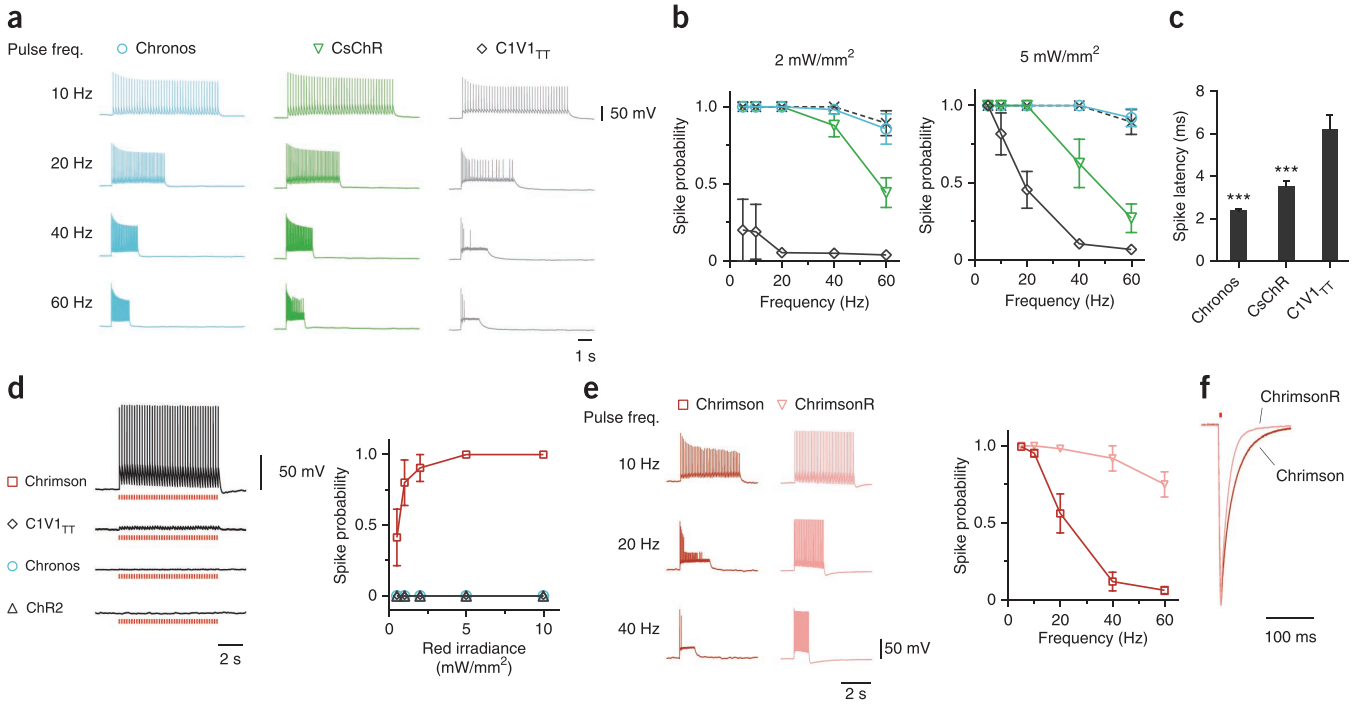

Figure 2 | Comparison of optical spiking in cultured neurons expressing different channelrhodopsins. (**a**–**c**) Green light–driven spiking fidelity. All green light spiking protocols used a train of 40 pulses, 2-ms pulse width, at 530 nm and at the indicated power (n = 5–8 cells for each opsin). (**a**) Representative green light–driven spiking traces at the indicated frequencies at 5 mW/mm^2. (**b**) Green light–driven spike probability over a range of frequencies. The dashed line is the electrical spiking control from Chronos-expressing neurons (this control comprised a train of 40 pulses at the indicated frequencies; each current-injection pulse was 5 ms long and was varied from 200 to 800 pA depending on each neuron's spike threshold). (**c**) Spike latencies (time between the light-pulse onset and the spike peak) calculated for 5-Hz trains at 5 mW/mm^2. (**d**–**f**) Comparison of spiking driven by red light (625 nm). (**d**) Representative current-clamp traces of red light response and spike fidelity (n = 5–8 cells for each opsin; 5-ms pulses, 5 Hz, 5 mW/mm^2). (**e**) Comparison of wild-type Chrimson and Chrimson K176R mutant (ChrimsonR) high-frequency red light spiking (n = 10 and 4 cells, respectively; 40-pulse train, 2-ms pulse width, 5 mW/mm^2). (**f**) Representative off-kinetics traces for Chrimson and ChrimsonR. ***P < 0.001; P = 0.0007 for CsChR and P < 0.0001 for Chronos; ANOVA with Dunnett's *post hoc* test with C1V1$_{TT}$ as reference. Plotted data are mean ± s.e.m.

(720 nm) also triggered EJPs (**Fig. 3c**); however, high-intensity light (1 mW/mm^2) and long light-pulse durations (40–160 ms) were required for robust activation of the NMJ (**Fig. 3d**,**e**). As a control, we tested a commonly used first-generation ChR2-expressing transgenic fly (ref. 33) and examined responses to 470-nm and 617-nm light pulses. As in previous work, 470-nm light triggered EJPs in ChR2-expressing animals, but only after relatively long light pulses (16 ms); 617-nm light pulses did not trigger EJPs in ChR2 animals (**Supplementary Fig. 14**).

In adult flies, we expressed Chrimson in sweet taste receptor cells (using the Gr64f-Gal4 line to drive its expression in the proboscis and legs[34]) and measured the proboscis extension reflex (PER) elicited by light stimulation at different wavelengths and intensities (**Supplementary Video 1** and **Supplementary Fig. 15**). At 470 nm and 617 nm, PERs were robust at very low light intensities (0.02 mW/mm^2 and 0.015 mW/mm^2, respectively; **Fig. 3f**). Flies also responded to 720-nm light at an intensity substantially lower than that required in the larvae (0.07 mW/mm^2, 10 ms; **Fig. 3f** and **Supplementary Video 2**). 720 nm is believed to be outside of the fly photoreceptor light-absorption spectra[35,36]; we therefore hypothesized that Chrimson could be used without inducing visually driven behavioral artifacts. However, control flies showed a clear startle response to 720-nm stimuli in darkness (**Fig. 3h** and **Supplementary Video 3**). Nevertheless, we reasoned that the saliency of 720-nm light would drop if it were presented along with other visual stimuli at a wavelength well within the sensitivity of photoreceptors, as might be expected during visual behavior experiments in adult flies. As expected, the startle response was efficiently inhibited when we introduced flowing blue random dots during 720-nm stimulation (reduction from 93.2% nonzero startle responses, out of 44 valid trials in darkness, to 22.2% out of 45 in a circular arena displaying flowing dots; see Online Methods for statistics), and the PER of Gr64f-Gal4/Chrimson-expressing flies was preserved (**Fig. 3g** and **Supplementary Videos 4** and **5**). With a far red–shifted activation spectrum, Chrimson also allows direct brain stimulation without removing the cuticle while animals freely behave. We expressed Chrimson in a set of antennal lobe projection neurons (PNv-1 using the VT03194-Gal4 driver line) innervating the V glomerulus, which is known to respond to CO_2 and induces an avoidance response when activated[37]. In this nonvisual paradigm, flies in a circular arena reliably avoided quadrants lit by weak red light (617 nm, 0.015 mW/mm^2; **Supplementary Fig. 16** and **Supplementary Video 6**; paired t-test: P = 0.007; see Online Methods), whereas wild-type flies did not show a response (P = 0.502).

Principles of two-color independent neural excitation

The fundamental limitation in creating an independent two-color channelrhodopsin pair is that all opsins can be driven to some extent by blue light. Additionally, neuron-to-neuron variation in opsin expression and optical scattering and absorption in tissue suggest that a large difference in effective blue light sensitivity

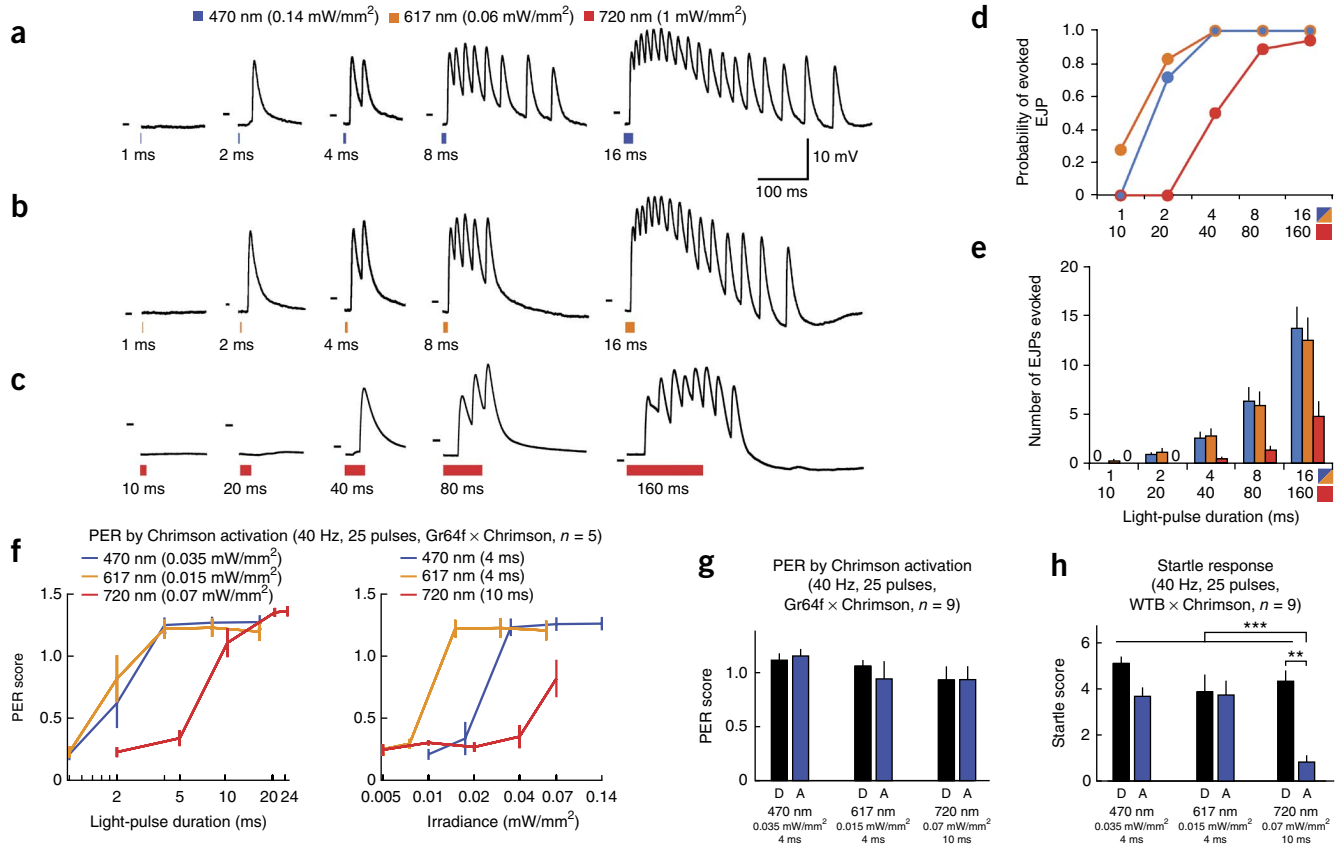

Figure 3 | Chrimson evokes action potentials in larval *Drosophila* motor neurons and triggers stereotyped behavior in adult *Drosophila*. (**a**–**c**) Intracellular recordings from m6 muscles in 3rd instar larvae expressing Chrimson in motor neurons. Responses to 470-nm, 617-nm and 720-nm light pulses of indicated power and increasing duration are shown. Dashes in each subpanel indicate −50 mV. (**d**) Probability of light-evoked excitatory junction potentials (EJPs) after pulses of 1, 2, 4, 8 or 16 ms in response to 470-nm and 617-nm light and after pulses of 10, 20, 40, 80 or 160 ms in response to 720-nm light. $n = 6$ muscles in 3 animals for all larvae experiments. (**e**) Mean number of EJPs evoked in response to light pulses. (**f**–**h**) Behavioral response of adult flies to light ($n = 5$ flies in each case). (**f**) Proboscis extension reflex (PER) of flies (pUAS-Chrimson-mVenus in attP18/*w*⁻;*Gr64f-GAL4*/+; *Gr64f-GAL4*/+, shown as Gr64f × Chrimson) in response to 25 pulses of lights at 470 nm, 617 nm and 720 nm (see Online Methods for PER scoring). (**g**) PER of Gr64f × Chrimson flies to pulsed light in darkness (D) or in a visual arena with flowing blue random dots (A). (**h**) Startle response of control flies (pUAS-Chrimson-mVenus in attP18/+;+/+;+/+, shown as WTB × Chrimson) to visual stimuli as in **g**. The startle score is the number of moving legs after stimulation. ***$P < 0.001$, **$P < 0.01$. Error bars, s.e.m.

between blue and red-shifted channelrhodopsins, in addition to a large spectral separation, is required to guarantee robust, independent spiking in mammalian brain tissue. We here systematically explored channelrhodopsins' blue light sensitivity in cultured neurons, where, unlike in intact brain tissue, it is possible to precisely control light power.

In evaluating potential blue partners, we first examined the importance of fast channelrhodopsin kinetics. When Chrimson is exposed to blue light levels as dim as 0.1 mW/mm^2 over long durations, as a slow-to-activate blue channelrhodopsin might require, charge integration can result in action potentials (**Fig. 4a**). However, the on-kinetics of Chronos are roughly three times faster than those of ChR2 and ten times faster than those of Chrimson across all blue irradiances tested (**Fig. 4d**), which suggests it may be possible to activate Chronos without substantially activating Chrimson.

Thus, we examined expression variation in Chrimson cells (**Fig. 4b**), as this variance will translate into some cells exhibiting larger blue light depolarizations than others. We found cross-talk of up to 25 mV at typical blue light powers used for ChR2 excitation (1 mW/mm^2, 470 nm, 5-ms pulse). Given Chronos's high photocurrent (**Fig. 1c**), high light sensitivity (**Fig. 4c**) and fast on- and off-kinetics (**Figs. 1f,g** and **4d**), we examined whether these properties would translate into spiking at low blue irradiances. Chronos reliably drove 100% spiking at light powers as low as 0.05 mW/mm^2 and maintained this fidelity over two orders of magnitude to 20 mW/mm^2 (**Fig. 4e,f**). When we determined the minimum irradiance threshold to achieve 100% spiking (MIT_{100}), Chronos had a consistently lower MIT_{100} than ChR2 for similar GFP fluorescence levels (**Fig. 4f** and **Supplementary Fig. 17**), a result suggesting that Chronos's high effective light sensitivity is not due to higher expression and that Chronos can robustly mediate light-sensitive control of neural spiking across a range of expression levels (**Fig. 4f**) without altering neural excitability (**Fig. 4g**). These properties make Chronos an ideal blue candidate to be combined with Chrimson.

Validation of two-color excitation in brain slices

To determine acceptable blue and red irradiances to selectively drive Chronos and Chrimson without spiking cross-talk, we first examined the powers at which 470-nm and 625-nm LEDs could drive spiking in Chronos and Chrimson neurons as well as the

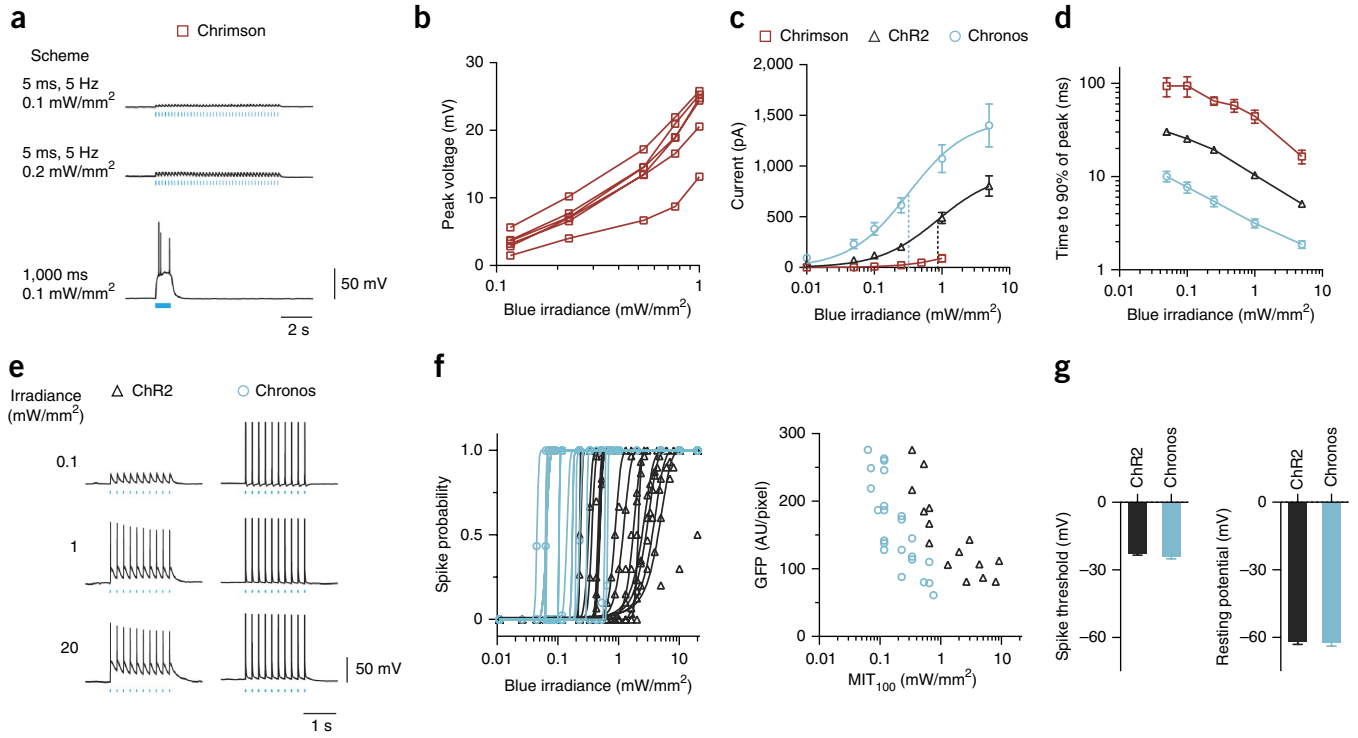

Figure 4 | Characterization of channelrhodopsin blue light (470-nm) sensitivities for two-color excitation in cultured neurons. (**a**) Current-clamp traces of representative Chrimson-expressing neuron under pulsed vs. continuous illumination. (**b**) Chrimson blue light–induced cross-talk voltages vs. irradiances for individual cells under pulsed illumination (5 ms, 5 Hz, $n = 5$ cells). (**c**) Photocurrent vs. blue irradiances (5-ms pulses; $n = 4$ cells for Chrimson, $n = 8$–10 cells for others). Vertical dashed lines indicate half-maximal points up the curves for ChR2 and Chronos as fitted. (**d**) Turn-on kinetics (1-s pulse; $n = 4$–7 cells; see **Supplementary Fig. 17b,c** for raw traces). (**e**–**g**) Comparison between ChR2 and Chronos spike probability over three logs of blue irradiance. All pulsed illuminations used 10 pulses, 5 Hz, 5 ms pulse width. (**e**) Representative spiking traces at the indicated irradiances. (**f**) Spike probability vs. blue light irradiance, plotted for individual Chronos- or ChR2-expressing neurons and minimum irradiance threshold for 100% spiking (MIT_{100}) as a function of GFP fluorescence. AU, arbitrary units. (**g**) Neuron spike threshold and resting potentials ($n = 16$–23 cells). Error bars, s.e.m.

conditions at which spike-level cross-talk occurred (**Fig. 5a–e**). We expressed Chrimson or Chronos in mouse cortical (layer 2/3) neurons via *in utero* electroporation and measured spike probabilities in opsin-expressing neurons in acute brain slices. As expected, we found that red light elicited spikes in only Chrimson-expressing cells (**Fig. 5c**) and blue light elicited spikes in Chronos-expressing cells using light powers as low as 0.05 mW/mm^2 (**Fig. 5d**). Chrimson-expressing neurons began to spike in response to blue light only when light powers were above 0.5 mW/mm^2 (**Fig. 5d**). This suggests that Chronos-expressing neurons can be driven with high fidelity without inducing spikes in Chrimson-expressing cells when using blue light irradiances between 0.2 and 0.5 mW/mm^2. Throughout this operational blue range, Chrimson-expressing cells showed subthreshold membrane depolarization events in response to blue light (**Fig. 5e**) comparable to the culture data (**Fig. 4b**).

We expressed Chrimson and Chronos in independent sets of neurons within the same cortical microcircuit in layer 2/3 neurons by electroporating Cre-on and Cre-off vectors[38]. To measure the synaptic output signal from the two targeted populations, we patch-clamped postsynaptic non-opsin-expressing neurons and measured optically evoked postsynaptic currents (PSCs) (**Fig. 5f–h**). For these experiments we chose a blue irradiance of 0.3 mW/mm^2 to elicit 100% Chronos spiking without Chrimson activation, and we used red irradiances of 1–4 mW/mm^2 to reliably activate Chrimson. We observed distinct PSC amplitudes when the cells were activated at the different wavelengths and light intensities (**Fig. 5i** and **Supplementary Figs. 18e** and **19a–c**). To examine whether these postsynaptic responses were cross-talk free at the synaptic transmission level, just as spiking events were at the action potential level, we singly expressed each opsin in distinct mouse brains, and we patch-clamped cells postsynaptic to opsin-expressing cells (**Fig. 5j–m** and **Supplementary Figs. 19d–g** and **20**). As expected, Chronos reliably drove synaptic events in response to blue light and never under red light (**Fig. 5k**; $P = 0.1$, paired t-test of peak current 30 ms before vs. 30 ms after red light delivery). Chrimson-expressing neurons reliably drove synaptic events upon red illumination and never upon blue illumination (**Fig. 5l**; $P = 0.43$, paired t-test of current before vs. after blue light delivery). Blue light–induced PSCs by Chrimson-expressing neurons began only outside this range, at 0.65 mW/mm^2 (**Fig. 5m**). We thus conclude it is possible to independently drive Chronos and Chrimson at the neural synaptic transmission level by using light powers determined by the operational blue irradiance range. As a final demonstration of Chronos's experimental utility, we found that pure axonal Chronos stimulation of retinal ganglion cell axons in the superior colliculus reliably elicited PSCs in downstream neurons (**Supplementary Fig. 21**).

DISCUSSION

We here present the results from a broad systematic screen of 61 algal opsins, sequenced *de novo* as part of a massive plant

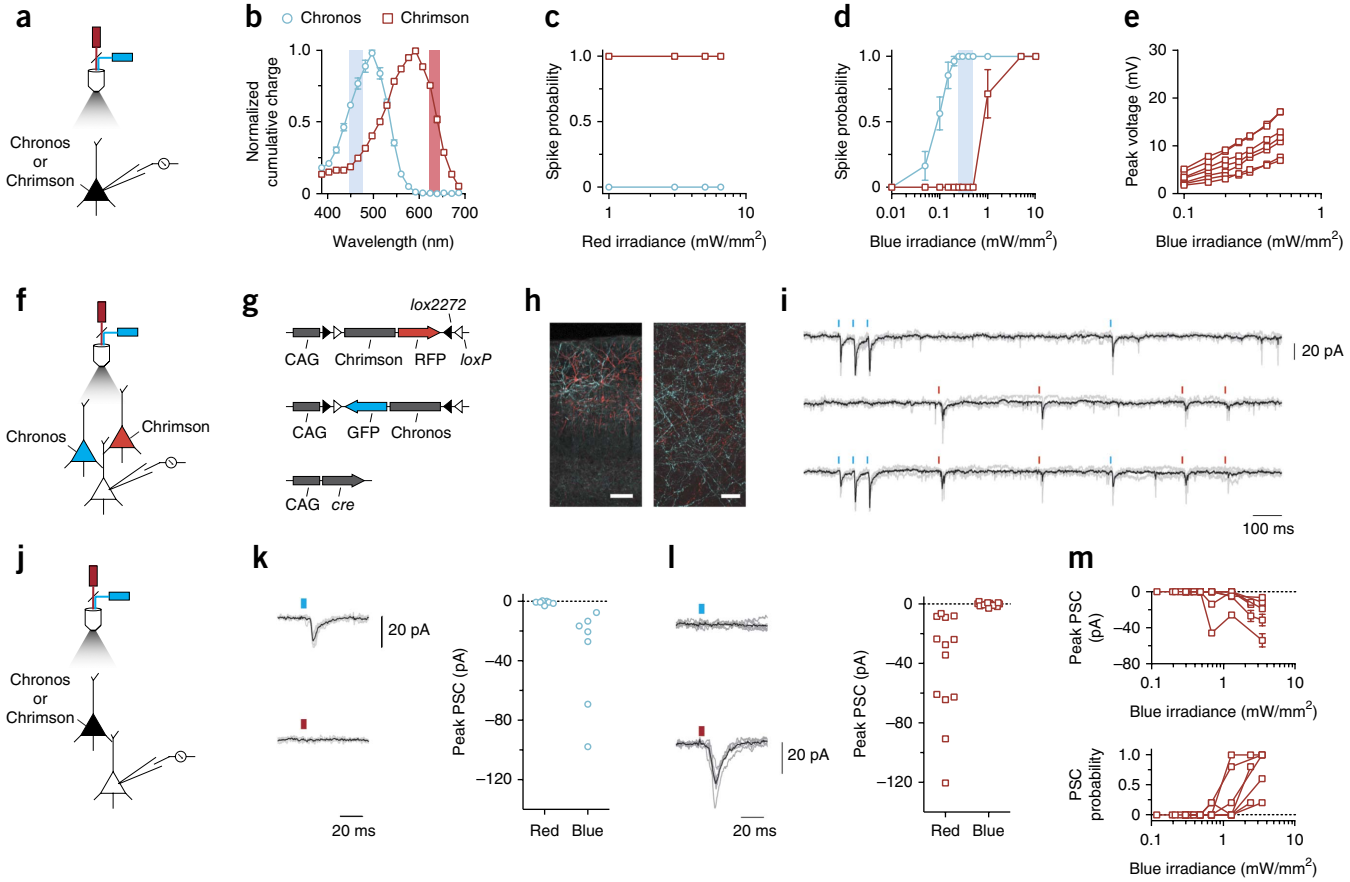

Figure 5 | Independent optical excitation of neural populations in mouse cortical slice using Chrimson and Chronos. (**a**–**e**) Spike and cross-talk characterization in opsin-expressing cells. Experimental optical configurations are depicted in **a**,**f**,**j**. (**b**) Chrimson and Chronos action spectra emphasizing (vertical shaded bars) the blue (470-nm) and red (625-nm) wavelengths used in this figure. (**c**–**e**) Current-clamp characterizations of Chrimson or Chronos expressing neurons in slice to determine optimal irradiance range for two-color excitation. Chrimson-GFP and Chronos-GFP were independently expressed in cortical layer 2/3 neurons in separate mice. 5-ms, 5-Hz light pulses were used; $n = 7$ cells from 3 animals for Chrimson; $n = 11$ cells from 4 animals for Chronos. (**c**,**d**) Spike probability vs. irradiance for red (**c**) and blue light (**d**). The blue vertical shaded bar represents the blue irradiance range where Chronos drove spikes at 100% probability and no cross-talk spike was ever observed for any Chrimson neurons. (**e**) Chrimson subthreshold cross-talk voltage in individual neurons vs. blue irradiances; compare to **Figure 4b**. (**f**–**i**) Postsynaptic currents (PSCs) in non-opsin-expressing neurons downstream of Chrimson and Chronos expressing neurons in brain slice with both opsins introduced into separate neural populations. Stimulation parameters: 0.3 mW/mm^2 for blue, 4 mW/mm^2 for red, 5-ms pulses; 6 neurons from 3 animals. All synaptic transmission slice experiments were done using wide-field illumination (**Supplementary Fig. 18**). (**g**) Triple-plasmid electroporation scheme for mutually exclusive Chrimson and Chronos expression in different sets of layer 2/3 cortical pyramidal cells. (**h**) Histology of intermingled Chrimson- (red) and Chronos-expressing (blue) neurons in layer 2/3 (left, taken at 10× magnification) and their axons (right, taken at 60× magnification). Scale bars: 100 µm (left), 20 µm (right). (**i**) PSCs in response to optical Poisson stimulation with blue and red light; shown are raw voltage traces (gray) with average trace (black) from a single neuron experiencing blue (top), red (center) or both (bottom) light pulses. (PSC traces from neurons downstream of mutually exclusive Chrimson- and Chronos-expressing neurons in response to blue or red light are in **Supplementary Fig. 18e**.) (**j**–**m**) PSCs in non-opsin-expressing neurons downstream of Chronos- or Chrimson-expressing neurons. Conditions are as in **f**–**i**, except pulses were delivered at 0.2 Hz. $n = 7$ cells from 2 animals for Chronos; $n = 12$ cells from 4 animals for Chrimson. The black trace is the averaged response; gray traces are individual trials. (**k**) Chronos-driven PSCs under blue or red light, obtained from a representative neuron (left), with population data (right). (**l**) Chrimson-driven PSCs under blue or red light traces, obtained from a representative neuron (left), with population data (right). (**m**) Chrimson-driven PSC amplitudes (top) and the probability of observing a PSC at all (bottom) vs. blue irradiances.

transcriptome endeavor[20] (http://www.onekp.com/). We discovered Chronos, an ultra-light-sensitive blue channelrhodopsin with faster kinetics than previously described opsins and which might represent an excellent general-use channelrhodopsin. We also discovered Chrimson, a red light–drivable channelrhodopsin 45 nm more red shifted than any previous channelrhodopsin and which might be useful in scenarios in which red light stimulation is essential. Previous channelrhodopsins that can be driven off-peak by red light (630 nm) have on-off kinetics exceeding 100 ms (refs. 9,14): perhaps a limitation of their original VChR1 scaffold. The spectral and kinetic properties of Chrimson and Chronos will enable fundamentally new types of experiments.

We explored the utility of Chrimson with red light in *D. melanogaster*. Chrimson was able to mediate responses in larval and adult flies with extremely low light powers across all wavelengths tested, most likely owing to the high expression achieved with the expression cassette used (see Online Methods). Further, light-induced startle responses of adult flies were significantly reduced at longer wavelengths (720 nm) when visual distractors of shorter wavelength were provided. Thus, Chrimson may be

useful for temporally precise neuronal stimulation in *Drosophila* behavioral experiments. Curiously, our results suggest that the photosensitivity of the fly eye extends well beyond the wavelength of typical room light for fly experiments (~650 nm), highlighting the utility of the 720-nm stimulation protocol we introduce for a wider range of behavioral experiments. Wavelengths lower than 720 nm will be useful in situations in which startle responses do not affect measurements of the parameters under study, such as stimulating neurons in the brain through intact cuticle to induce nonvisually driven behaviors as here shown with 617-nm light and CO_2-responding neurons, something that has not yet been reliably demonstrated using optogenetic techniques. The ability to perform optogenetic behavioral experiments in intact flies with Chrimson at redder wavelengths than ReaChR[14,29], due to the ~45-nm spectral shift, may permit lower light levels to be used and reduce visual system–mediated artifacts.

Using both Chronos and Chrimson, we found an ample blue light irradiance range that evoked reliable Chronos-induced spikes without any Chrimson-induced spikes in mouse cortical slice and that also allowed Chronos-induced synaptic transmission without any Chrimson-induced synaptic transmission. As most two-color experimental setups will not be identical to our slice demonstration, several constraints exist upon the use of effective blue light sensitivity to achieve two-color separation. Whenever possible, Chronos should be expressed under the stronger promoter and the more excitable neuron type to minimize Chrimson-induced depolarization. The experiments in this paper characterized two-color excitation with symmetric promoters and cell types to stringently test whether Chronos and Chrimson can, without exploiting differences in cellular excitability, present a clear separation due to biophysical properties. Neuroscientists seeking to manipulate two different cell populations may find that expressing Chronos at high levels in the more excitable cell type may further increase the reliable blue dynamic range.

Although Chronos has the fastest kinetic properties among reported channelrhodopsins, blue light pulses delivered at very high frequencies as part of a two-color experiment could in principle lead to charge integration and, thus, to Chrimson blue spiking cross-talk. The temporal precision of Chronos- versus Chrimson-mediated synaptic events may also depend on light power, potentially limiting usage in scenarios requiring submillisecond timing of synaptic release, although ~1-ms jitter is achievable. We have additionally observed in postsynaptic experiments that the stimulation frequency for both red and blue pulses is fundamentally limited by the wild-type Chrimson, the slowest of the opsin pair. This is why we engineered ChrimsonR, a faster Chrimson kinetic mutant, which has similar blue light sensitivity to the wild type but allows modulation at above the 20-Hz range. It may be desirable to further improve Chrimson's kinetics and decrease its light sensitivity to enable high-frequency modulation in both the red and blue channels and to increase the usable blue irradiance range.

For applications *in vivo*, it would be important to illuminate the circuit region of interest with powers that fall within the windows here defined; for mammals, one might use alternative illumination methods such as three-dimensional optical waveguides[39] or wireless LED implants[40]. Although these constraints add complexity to experiments, they may also enable *in vivo* two-color experiments not previously possible.

METHODS

Methods and any associated references are available in the online version of the paper.

Accession codes. GenBank/EMBL/DDBJ: new channelrhodopsins identified here are listed under accession codes KF992030–KF992090; see also **Supplementary Table 1**.

Note: Any Supplementary Information and Source Data files are available in the online version of the paper.

ACKNOWLEDGMENTS

We thank A. Karpova (Janelia Farm) for technical advice, reagents and generous assistance with construct preparation for *Drosophila*; K. Hibbard and members of the Janelia Fly Core for fly husbandry and assistance with fly crosses; and J. Pulver for technical advice and assistance with data analysis software. We thank Y. Aso, W. Ming and G. Rubin (Janelia Farm) for kindly allowing us to use their circular light arena and for useful discussion. We thank I. Negrashov, S. Sawtelle and J. Liu for arena-related development and support. We thank J.R. Carlson (Yale University) for Gr64f-Gal4 flies, W.D. Tracey Jr. (Duke University) for UAS-Chr2 flies, G.M. Rubin (Janelia Farm) for pBDP-Gal4 flies and B.J. Dickson (IMP, Vienna and Janelia Farm) for VT031497-Gal4 flies.

S.S.K., S.R.P. and V.J. were supported by the Howard Hughes Medical Institute. The 1000 Plants (1KP) initiative, led by G.K.-S.W., is funded by the Alberta Ministry of Enterprise and Advanced Education, Alberta Innovates Technology Futures (AITF) Innovates Centre of Research Excellence (iCORE), Musea Ventures, and BGI-Shenzhen. B.Y.C. and E.S.B. were funded by Defense Advanced Research Projects Agency (DARPA) Living Foundries HR0011-12-C-0068. B.Y.C. was funded by the US National Science Foundation (NSF) Biophotonics Program. M.C.-P. was funded by US National Institutes of Health (NIH) grant 5R01EY014074-18. E.S.B. was funded by the MIT Media Lab, Office of the Assistant Secretary of Defense for Research and Engineering, Harvard/MIT Joint grants in Basic Neuroscience, NSF (especially CBET 1053233 and EFRI 0835878), NIH (especially 1DP2OD002002, 1R01NS067199, 1R01DA029639, 1R01GM104948, 1RC1MH088182 and 1R01NS075421), Wallace H. Coulter Foundation, Alfred P. Sloan Foundation, Human Frontiers Science Program, New York Stem Cell Foundation Robertson Neuroscience Investigator Award, Institution of Engineering and Technology A.F. Harvey Prize, and Skolkovo Institute of Science and Technology.

AUTHOR CONTRIBUTIONS

N.C.K., E.S.B., M.C.-P. and V.J. contributed to the study design and data analysis. G.K.-S.W. and B.Y.C. oversaw transcriptomic sequencing. E.S.B. and M.C.-P. supervised mammalian opto/electrophysiological parts of the project. N.C.K. coordinated all experiments and data analysis. N.C.K., Y.K.C., A.S.C. and T.K.M. conducted and analyzed all *in vitro* electrophysiology. M.M., B.S., N.C.K., T.K.M., E.J.C., Z.T., J.W., Y.X., Z.Y. and Y.Z. conducted algal RNA experiments or transcriptome sequencing and analysis. N.C.K., Y.M. and A.B.-B. performed and analyzed all slice electrophysiology. V.J. prepared Chrimson for injection into *Drosophila*. S.S.K. and V.J. designed adult fly behavior experiments. S.S.K. performed all fly behavior experiments and data analysis. S.R.P. designed, performed and analyzed all larval *Drosophila* experiments. Correspondence should be addressed to V.J. (vivek@janelia.hhmi.org) for Chrimson flies. All authors contributed to the discussions and writing of the manuscript.

COMPETING FINANCIAL INTERESTS

The authors declare competing financial interests: details are available in the online version of the paper.

1. Boyden, E.S., Zhang, F., Bamberg, E., Nagel, G. & Deisseroth, K. Millisecond-timescale, genetically targeted optical control of neural activity. *Nat. Neurosci.* **8**, 1263–1268 (2005).
2. Han, X. & Boyden, E.S. Multiple-color optical activation, silencing, and desynchronization of neural activity, with single-spike temporal resolution. *PLoS ONE* **2**, e299 (2007).
3. Chow, B.Y. *et al.* High-performance genetically targetable optical neural silencing by light-driven proton pumps. *Nature* **463**, 98–102 (2010).
4. Zhang, F. *et al.* Multimodal fast optical interrogation of neural circuitry. *Nature* **446**, 633–639 (2007).

5. Gradinaru, V. *et al.* Molecular and cellular approaches for diversifying and extending optogenetics. *Cell* **141**, 154–165 (2010).
6. Boyden, E.S. A history of optogenetics: the development of tools for controlling brain circuits with light. *F1000 Biol. Rep.* **3**, 11 (2011).
7. Zhang, F. *et al.* Red-shifted optogenetic excitation: a tool for fast neural control derived from Volvox carteri. *Nat. Neurosci.* **11**, 631–633 (2008).
8. Erbguth, K., Prigge, M., Schneider, F., Hegemann, P. & Gottschalk, A. Bimodal activation of different neuron classes with the spectrally red-shifted channelrhodopsin chimera C1V1 in *Caenorhabditis elegans*. *PLoS ONE* **7**, e46827 (2012).
9. Yizhar, O. *et al.* Neocortical excitation/inhibition balance in information processing and social dysfunction. *Nature* **477**, 171–178 (2011).
10. Prigge, M. *et al.* Color-tuned channelrhodopsins for multiwavelength optogenetics. *J. Biol. Chem.* **287**, 31804–31812 (2012).
11. Wang, W. *et al.* Tuning the electronic absorption of protein-embedded all-trans-retinal. *Science* **338**, 1340–1343 (2012).
12. Waddell, W.H., Schaffer, A.M. & Becker, R.S. Visual pigments. 3. Determination and interpretation of the fluorescence quantum yields of retinals, Schiff bases, and protonated Schiff bases. *J. Am. Chem. Soc.* **95**, 8223–8227 (1973).
13. Govorunova, E.G., Spudich, E.N., Lane, C.E., Sineshchekov, O.A. & Spudich, J.L. New channelrhodopsin with a red-shifted spectrum and rapid kinetics from *Mesostigma viride*. *mBio* **2**, e00115–e00111 (2011).
14. Lin, J.Y., Knutsen, P.M., Muller, A., Kleinfeld, D. & Tsien, R.Y. ReaChR: a red-shifted variant of channelrhodopsin enables deep transcranial optogenetic excitation. *Nat. Neurosci.* **16**, 1499–1508 (2013).
15. Kleinlogel, S. *et al.* Ultra light-sensitive and fast neuronal activation with the Ca^{2+}-permeable channelrhodopsin CatCh. *Nat. Neurosci.* **14**, 513–518 (2011).
16. Berndt, A., Yizhar, O., Gunaydin, L.A., Hegemann, P. & Deisseroth, K. Bi-stable neural state switches. *Nat. Neurosci.* **12**, 229–234 (2009).
17. Bamann, C., Gueta, R., Kleinlogel, S., Nagel, G. & Bamberg, E. Structural guidance of the photocycle of channelrhodopsin-2 by an interhelical hydrogen bond. *Biochemistry* **49**, 267–278 (2010).
18. Mattis, J. *et al.* Principles for applying optogenetic tools derived from direct comparative analysis of microbial opsins. *Nat. Methods* **9**, 159–172 (2012).
19. Govorunova, E.G., Sineshchekov, O.A., Li, H., Janz, R. & Spudich, J.L. Characterization of a highly efficient blue-shifted channelrhodopsin from the marine alga *Platymonas subcordiformis*. *J. Biol. Chem.* **288**, 29911–29922 (2013).
20. Johnson, M.T. *et al.* Evaluating methods for isolating total RNA and predicting the success of sequencing phylogenetically diverse plant transcriptomes. *PLoS ONE* **7**, e50226 (2012).
21. Lin, J.Y. A user's guide to channelrhodopsin variants: features, limitations and future developments. *Exp. Physiol.* **96**, 19–25 (2011).
22. Nagel, G. *et al.* Light activation of channelrhodopsin-2 in excitable cells of *Caenorhabditis elegans* triggers rapid behavioral responses. *Curr. Biol.* **15**, 2279–2284 (2005).
23. de Vries, S.E. & Clandinin, T.R. Loom-sensitive neurons link computation to action in the *Drosophila* visual system. *Curr. Biol.* **22**, 353–362 (2012).
24. Schroll, C. *et al.* Light-induced activation of distinct modulatory neurons triggers appetitive or aversive learning in *Drosophila* larvae. *Curr. Biol.* **16**, 1741–1747 (2006).
25. Gaudry, Q., Hong, E.J., Kain, J., de Bivort, B.L. & Wilson, R.I. Asymmetric neurotransmitter release enables rapid odour lateralization in *Drosophila*. *Nature* **493**, 424–428 (2013).
26. Honjo, K., Hwang, R.Y. & Tracey, W.D. Jr. Optogenetic manipulation of neural circuits and behavior in *Drosophila* larvae. *Nat. Protoc.* **7**, 1470–1478 (2012).
27. Zhang, W., Ge, W. & Wang, Z. A toolbox for light control of *Drosophila* behaviors through Channelrhodopsin 2-mediated photoactivation of targeted neurons. *Eur. J. Neurosci.* **26**, 2405–2416 (2007).
28. Xiang, Y. *et al.* Light-avoidance-mediating photoreceptors tile the *Drosophila* larval body wall. *Nature* **468**, 921–926 (2010).
29. Inagaki, H.K. *et al.* Optogenetic control of *Drosophila* using a red-shifted channelrhodopsin reveals experience-dependent influences on courtship. *Nat. Methods* doi:10.1038/nmeth.2765 (22 December 2013).
30. Claridge-Chang, A. *et al.* Writing memories with light-addressable reinforcement circuitry. *Cell* **139**, 405–415 (2009).
31. Pulver, S.R., Pashkovski, S.L., Hornstein, N.J., Garrity, P.A. & Griffith, L.C. Temporal dynamics of neuronal activation by Channelrhodopsin-2 and TRPA1 determine behavioral output in *Drosophila* larvae. *J. Neurophysiol.* **101**, 3075–3088 (2009).
32. Bernstein, J.G., Garrity, P.A. & Boyden, E.S. Optogenetics and thermogenetics: technologies for controlling the activity of targeted cells within intact neural circuits. *Curr. Opin. Neurobiol.* **22**, 61–71 (2012).
33. Hwang, R.Y. *et al.* Nociceptive neurons protect *Drosophila* larvae from parasitoid wasps. *Curr. Biol.* **17**, 2105–2116 (2007).
34. Dahanukar, A., Lei, Y.T., Kwon, J.Y. & Carlson, J.R. Two *Gr* genes underlie sugar reception in *Drosophila*. *Neuron* **56**, 503–516 (2007).
35. Minke, B. & Kirschfeld, K. The contribution of a sensitizing pigment to the photosensitivity spectra of fly rhodopsin and metarhodopsin. *J. Gen. Physiol.* **73**, 517–540 (1979).
36. Salcedo, E. *et al.* Blue- and green-absorbing visual pigments of *Drosophila*: ectopic expression and physiological characterization of the R8 photoreceptor cell-specific Rh5 and Rh6 rhodopsins. *J. Neurosci.* **19**, 10716–10726 (1999).
37. Lin, H.H., Chu, L.A., Fu, T.F., Dickson, B.J. & Chiang, A.S. Parallel neural pathways mediate CO_2 avoidance responses in *Drosophila*. *Science* **340**, 1338–1341 (2013).
38. Atasoy, D., Aponte, Y., Su, H.H. & Sternson, S.M. A FLEX switch targets Channelrhodopsin-2 to multiple cell types for imaging and long-range circuit mapping. *J. Neurosci.* **28**, 7025–7030 (2008).
39. Zorzos, A.N., Scholvin, J., Boyden, E.S. & Fonstad, C.G. Three-dimensional multiwaveguide probe array for light delivery to distributed brain circuits. *Opt. Lett.* **37**, 4841–4843 (2012).
40. Kim, T.I. *et al.* Injectable, cellular-scale optoelectronics with applications for wireless optogenetics. *Science* **340**, 211–216 (2013).

ONLINE METHODS

Opsins and species. Key opsins are abbreviated throughout the paper and figures as follows, with species or derivation listed in parentheses: VChR1 (*Volvox carteri*), $C1V1_{TT}$ (VChR1/ChR1 chimera), ChR1 (*Chlamydomonas reinhardtii*), CsChR (*Chloromonas subdivisa*), AgChR (*Asteromonas gracillis-B*), ChR2 (*Chlamydomonas reinhardtii*), CoChR (*Chloromonas oogama*), NsChR (*Neochlorosarcina* sp.), ShChR (*Stigeoclonium helveticum*; also called Chronos), MvChR1 (*Mesostigma viride*), SdChR (*Scherffelia dubia*), TsChR (*Tetraselmis striata*), TcChR (*Tetraselmis cordiformis*), BsChR (*Brachiomonas submarina*), CnChR (*Chlamydomonas noctigama*; also called Chrimson), HdChR (*Haematococcus droebakensis*), CbChR (*Chlamydomonas bilatus-A*), PsChR (*Proteomonas sulcata*). For a detailed list of all opsins found, their species of origin, and their GenBank accession numbers, see **Supplementary Table 1**.

Molecular cloning. All opsin genes were synthesized (Genscript) with mammalian codon optimization and subcloned as previously described[3]. $C1V1_{TT}$ and ReaChR were synthesized with the same codon usage as previously described[9,14]. For cultured neuron studies, all genes were subcloned into a lentiviral backbone under a CaMKII promoter and with a C-terminal GFP fusion. No trafficking sequences were added to any opsin-encoding genes. The tdTomato plasmid used for cotransfection in cultured neuron was also subcloned into a lentiviral backbone, but with a ubiquitin promoter instead. For *in utero* electroporation experiments, all genes were subcloned into pCAGIG vector (Addgene 11159) with C-terminal GFP, tdTomato, or mOrange2 fusion. The Cre-dependent vectors were generated using the same pCAGIG vector but with *lox* sites flanking the protein-coding region as done previously[38].

We performed RACE on some of the sequences (**Supplementary Fig. 1**) by using 5′ RNA ligation to enrich for full-length transcripts (**Supplementary Table 3**). This protocol is the same as in the Ambion RLM-RACE kit, and PCR primers were designed on the basis of partial transcriptome sequencing results. RACE products were blunt cloned (Invitrogen Zero Blunt kit) into a vector for Sanger sequencing.

Characterization of channel kinetics and ion selectivity in HEK293FT cells. Whole-cell patch-clamp recordings were performed in isolated HEK293FT cells to avoid space clamp issues. All recordings were performed using an Axopatch 200B amplifier and Digidata 1440 digitizer (Molecular Devices) at room temperature. To allow isolated cell recording, we plated cells at a density of 15,000 cells per well in 24-well plates that contained round glass coverslips (0.15 mm thick, 25 mm in diameter, coated with 2% growth factor–reduced Matrigel in DMEM for 1 h at 37 °C). To ensure accurate measurements, we used cells with access resistance <25 MΩ and holding current within ±50 pA. Typical membrane resistance was between 500 MΩ and 2 GΩ, and pipette resistance was between 3 and 6 MΩ. Photostimulation of patch-clamped cells was conducted with a 470-nm LED (Thorlabs) at irradiance of 10 mW/mm for ChR2, ChR2 E123A, and Chronos, and by a 590-nm LED (Thorlabs) at irradiance of 4.6 mW/mm for Chrimson.

For characterizing channel kinetics, the extracellular solution (Tyrode's solution) consisted of (in mM) 125 NaCl, 2 KCl, 3 $CaCl_2$, 1 $MgCl_2$, 10 HEPES, 30 glucose, pH 7.3 (NaOH adjusted), 305 mOsm; and the intracellular solution consisted of (in mM) 125 K-gluconate, 8 NaCl, 0.1 $CaCl_2$, 0.6 $MgCl_2$, 1 EGTA, 10 HEPES, 4 Mg-ATP, 0.4 Na-GTP, pH 7.3 (KOH adjusted), with 295–300 mOsm (sucrose adjusted). Channel closing rates (τ_{off}; for example, as in **Fig. 3a**) were measured by fitting the decay of photocurrent after 2-ms light pulses to monoexponential curves, and time to peak (time to reach 90% of peak photocurrent after the beginning of illumination, as in **Fig. 3b**) values were measured from 1-s pulses.

Ion selectivity characterization (**Supplementary Fig. 4**) was done using solutions listed in **Supplementary Table 4**. The liquid junction potentials were 5.8 mV and 4.9 mV for 90 mM $CaCl_2$ and 5 mM NaCl solutions, respectively, and were corrected during recording; the others were <1 mV in liquid junction potential. The peak component of the photocurrent during a 1-s illumination was used to calculate photocurrent density ratios.

HEK 293FT cell culture and transfection. HEK 293FT cells (Invitrogen) were maintained between 10% and 70% confluence in D10 medium (Cellgro) supplemented with 10% FBS (Invitrogen), 1% penicillin/streptomycin (Cellgro), and 1% sodium pyruvate (BioWhittaker). For recording, cells were plated at 5–20% confluence on glass coverslips coated with Matrigel (BD Biosciences). Adherent cells were transfected approximately 24 h post plating either with TransLT 293 Lipofectamine transfection kits (Mirus) or with calcium phosphate transfection kits (Invitrogen) and recorded via whole-cell patch clamp between 36 and 72 h post transfection. 1.25 μg of DNA was delivered. 1 μM of all-*trans*-retinal was supplemented to the culture medium for 1 h before patch-clamp experiments.

Primary neuron culture and transfection. All procedures involving animals were in accordance with the US National Institutes of Health Guide for the Care and Use of Laboratory Animals and approved by the Massachusetts Institute of Technology Committee on Animal Care. Hippocampal neuron culture was prepared from postnatal day 0 or day 1 Swiss Webster (Taconic or Charles River) mice as previously described[3] but with the following modifications: dissected hippocampal tissues were digested with 50 units of papain (Worthington Biochem) for 5 min, and the digestion was stopped with ovomucoid trypsin inhibitor (Worthington Biochem). Cells were plated at a density of 16,000–20,000 per glass coverslip coated with Matrigel (BD Biosciences).

Cultured neurons were transfected at 4 days *in vitro* (DIV) with a commercial calcium phosphate kit (Invitrogen). We added an additional washing with acidic MEM buffer (pH 6.8–6.9) after calcium phosphate precipitate incubation to completely resuspend residual precipitates[41]. tdTomato was used as a cotransfectant DNA reagent to assist with unbiased selection of opsin-expressing neurons (see main text); in this condition, we delivered 2 μg of opsin DNA and 0.2 μg tdTomato. When no tdTomato was used, we used 2 μg of opsin DNA alone.

Whole-cell electrophysiology *in vitro* and in slice. Whole-cell patch-clamp recordings were made using the Axopatch 200B or Multiclamp 700B amplifier, a Digidata 1440 digitizer, and a PC running pClamp (Molecular Devices). For *in vitro* current-clamp recordings, neurons were patched 14–18 DIV (10–14 d post

transfection) to allow for sodium channel maturation. Neurons were bathed in room-temperature Tyrode solution containing 125 mM NaCl, 2 mM KCl, 3 mM $CaCl_2$, 1 mM $MgCl_2$, 10 mM HEPES, 30 mM glucose, 0.01 mM NBQX and 0.01 mM GABAzine. The Tyrode pH was adjusted to 7.3 with NaOH, and the osmolarity was adjusted to 300 mOsm with sucrose. For *in vitro* voltage-clamp recordings, neurons were patched 11–14 DIV (7–10 d post transfection); the recording conditions here were similar to those for current-clamp recordings, except the Tyrode solution also contained 1 µM tetrodotoxin (TTX, Tocris Bioscience). No all-*trans*-retinal was supplemented for any cultured neuron recordings.

For slice recordings, room-temperature artificial cerebrospinal fluid (ACSF) was continuously perfused over slices, and no blockers were used. ACSF contained 127 mM NaCl, 2.5 mM KCl, 25 mM $NaHCO_3$, 1.25 mM NaH_2PO_4, 12 mM D-glucose, 0.4 mM sodium ascorbate, 2 mM $CaCl_2$, and 1 mM $MgCl_2$ and was bubbled continuously with 95% oxygen/5% CO_2.

For both *in vitro* and slice recordings, borosilicate glass pipettes (Warner Instruments) with an outer diameter of 1.2 mm and a wall thickness of 0.255 mm were pulled to a resistance of 3–7 MΩ with a P-97 Flaming/Brown micropipette puller (Sutter Instruments) and filled with a solution containing 125 mM K-gluconate, 8 mM NaCl, 0.1 mM $CaCl_2$, 0.6 mM $MgCl_2$, 1 mM EGTA, 10 mM HEPES, 4 mM Mg-ATP, and 0.4 mM Na-GTP. The pipette solution pH was adjusted to 7.3 with KOH, and the osmolarity was adjusted to 298 mOsm with sucrose. For voltage-clamp experiments, cells were clamped at −65 mV for *in vitro* (HEK293, cultured neuron) recordings and between −65 and −80 mV for slice recordings. For current-clamp experiments, <50-pA constant current injection was used for *in vitro* recordings, and no current injection was used for slice recordings. To ensure accurate measurements, we used cells with access resistance between 5 and 35 MΩ and holding current within ±100 pA (at −65 mV, in voltage clamp). Access resistance was monitored throughout recording. Data were analyzed using Clampfit (Molecular Devices) and custom Matlab scripts (MathWorks).

Light delivery and imaging. All neuron culture and slice experiments were done with the LEDs mounted on microscope for wide-field illumination, with nominal wavelength at 470 nm, 530 nm, 625 nm, 660 nm and 735 nm (Thorlabs, M470L2, M530L2, M625L3, M660L3 and M735L3 respectively). We additionally filtered LEDs spectrum with the following bandpass filters (Semrock): 530-nm LED with 543 ± 11 nm filter, 625-nm LED with 632 ± 11 nm, and 660-nm LED with 661 ± 10 nm. The 735-nm LED was not additionally filtered. Light power was controlled through the LED driver using analog voltage modulation (LEDD1B or DC4100, Thorlabs), and voltage pulse width was adjusted to obtain the desired illumination duration as measured with a photometer (S120VC, Thorlabs). Illumination spot size with different objectives was measured by focusing on a microscope slide coated with appropriate-wavelength Alexa dye and photobleaching it for 10 min under full-intensity illumination. The photobleached slide was then imaged with a micrometer calibration slide to determine the photobleached radius.

Action spectrum data were taken with a monochromator (Till-Photonics Polychrome IV, bandwidth 15 nm centered around each value), and a separate (Uniblitz) shutter was used to gate the light pulses to 10 ms. Equal photon fluxes of ~2.5×10^{21} photons/s/m^2 (~1.1 mW/mm^2 at 450 nm) were used across wavelengths by using the monochromator's built-in intensity adjustment. We additionally corrected for any photon dosage difference (12% at the most) between wavelengths by dividing the recorded opsin response by the measured photon dose. A (QuickMacros) script was used to automate the wavelength and intensity selections and to synchronize with electrophysiology recording. For each cell, wavelengths were swept from blue to red and from red to blue, and the responses were averaged.

Photocurrent measurements were single trial, and input resistance was monitored throughout. For color-ratio comparisons, the order of illumination wavelength was shuffled between different cells. For photocurrent recovery kinetics measurements, an additional 2-min wait in the dark preceded the protocol to allow for recovery before the measurement was begun. In protocols where irradiances (or stimulation frequencies) were varied, the irradiances (or stimulation frequencies) were either shuffled or measured both from low to high and high to low. In the acute slice postsynaptic experiments, at least five sweeps were taken for each condition.

Unless otherwise specified, all experiments included a 20- to 30-s wait in the dark between sweeps to allow for opsin recovery.

Quantitative fluorescence comparison of opsin-GFP and cytosolic tdTomato expressed in cultured neurons was imaged with Leica HCX APO L 20× objective (air, numerical aperture (NA) = 0.5) using Hamamatsu Orca Flash 2.8 under identical illumination conditions throughout: 445-nm LED (Thorlabs) at 4.28 mW/mm^2 using EN GFP filter cube (Leica) for GFP fluorescence; 530-nm LED (Thorlabs) with 543 nm ± 11 nm filter (Semrock) at 2.14 mW/mm^2 using Custom R filter cube (Leica) for tdTomato fluorescence.

***In utero* electroporation and virus delivery for acute slice experiments.** All procedures were in accordance with the National Institutes of Health Guide for the Care and Use of Laboratory Animals and approved by the Massachusetts Institute of Technology Committee on Animal Care. C57BL/6J E16-timed pregnant mice were used for electroporation. Surgery was done under ketamine-xylazine anesthesia and buprenorphine analgesia. For cortical experiments, DNA solution containing plasmids of interest was injected into the lateral ventricle of each embryo using a pulled capillary tube. Five square pulses (50-ms width, 1 Hz, 35 V) were applied using a tweezer electrode for electroporation (Harvard Apparatus, ECM 830). Brains of mice for experiments in which opsin-expressing cells were to be experimentally characterized were electroporated with pCAG-opsin-GFP plasmid. Brains of mice in which downstream, non-opsin-expressing neurons were to be experimentally characterized were electroporated with pCAG-FLEX-rc[Chronos-GFP] and/or pCAG-FLEX-Chrimson-mOrange2, and pCAG-Cre plasmids. pCAG-Chrimson-tdTomato was additionally used in half of the single postsynaptic experiments.

For the retinal ganglion cell–superior colliculus experiment, intravitreal virus injection was performed on P0 C57BL/6 mice with Nanoject II (Drummond) under cold anesthesia. 100 nL of rAAV2/8-Synapsin-Chronos-GFP (titer: 1.4×10^{13} particles/mL)

doi:10.1038/nmeth.2836

was injected into the eye. AAV particles were produced by the University of North Carolina Chapel Hill Vector Core.

Data analysis. Phylogenetic trees were generated using the neighbor-joining method with *p*-distance model (MEGA5).

Opsin-GFP and tdTomato fluorescence was measured with custom Matlab script using masks around neuron soma region. Masks were generated (on the basis of either GFP or tdTomato images) using CellProfiler (http://www.cellprofiler.org/) and manually edited in ImageJ to remove neuronal processes. The same mask was used to quantify both GFP and tdTomato fluorescence.

Action spectra were computed by integrating charge from light onset to the half-max time. Half-max time refers to the time that the highest amplitude response wavelength has half of its peak current. This is to ensure the measured response is the transition from ground state as opposed to secondary photoproducts. Given that the integration window is the same across wavelengths for a given cell (typically 1–3 ms), this is effectively measuring the initial slope as was done previously by other labs[13].

The points halfway up the curve (e.g., analogous to the pharmacology concept of EC_{50}) in **Figure 4c** were calculated by fitting 5-ms blue irradiance photocurrents to the one-site specific binding model ($y = B_{max} \times x/(K_d + x)$ using Prism (GraphPad Software), where the K_d corresponds to EC_{50} and B_{max} corresponds to the extrapolated maximum photocurrent at saturating irradiance. This is the same convention as previously published paper[18].

Spikes were defined as depolarizing above 0 mV and then repolarizing below −30 mV within each stimulation interval. Spike threshold was measured with a 500-ms current ramp (400–800 pA) current injection protocol and determined with custom Matlab script. Threshold was defined as the voltage at which the slope (dV/dt) has exceeded 0.3 mV/s.

Slice preparation. P20–P40 mice were used for slice preparation unless otherwise specified. Mice were anesthetized with isofluorane and transcardially perfused with ice-cold cutting solution containing 110 mM choline chloride, 25 mM $NaHCO_3$, 25 mM D-glucose, 11.6 mM sodium ascorbate, 7 mM $MgCl_2$, 3.1 mM sodium pyruvate, 2.5 mM KCl, 1.25 mM NaH_2PO_4, and 0.5 mM $CaCl_2$. The brain was then carefully removed and mounted in a vibrating-blade microtome (Leica VT1000S). 300-mm-thick coronal slices of the cortex (varying regions of brain were sectioned, depending on where the electroporation resulted in expressing neurons; they were as a rule found in layer 2/3 of the cortical area obtained) were cut with a vibrating metal blade at 90 Hz and 0.1 mm/s cutting speed. Sectioned slices were incubated in 37 °C cutting solution for 30–45 min before being transferred to room-temperature oxygenated artificial cerebrospinal fluid (ACSF) for recording. ACSF contained 127 mM NaCl, 2.5 mM KCl, 25 mM $NaHCO_3$, 1.25 mM NaH_2PO_4, 12 mM D-glucose, 0.4 mM sodium ascorbate, 2 mM $CaCl_2$, and 1 mM $MgCl_2$. For spiking characterization (**Fig. 5c–e**), we used a Nikon CFI Apo 60× NIR objective (water immersion, NA = 1); for synaptic characterizations (**Fig. 5f–m**), we used a Nikon CFI Super Plan Fluor ELWD 20xC objective (air, NA = 0.45) in order to recruit as many synapses as possible to insure stringency of the zero–cross-talk synaptic control. For slice experiments, electrical artifacts were apparent in the recorded traces as a result of LED on-off coupling to fluids flowing by the slice, as LED was in the Faraday cage; we include raw traces with artifacts interpolated in **Figure 5** and those without artifact interpolation in **Supplementary Figure 22**.

Fly stocks. Chrimson constructs were prepared with additional Golgi and ER export motifs[42–45] in the pJFRC7-20XUAS-IVS vector[46] and inserted in attP18/+;+/+;+/+. To express Chrimson in larval motor neurons, we crossed UAS-Chrimson-mVenus flies to flies containing a Gal4 driver (OK371-Gal4) that drives expression in all glutamatergic neurons[47]. We used the same Gal4 line to express ChR2 (ref. 33) in larval motor neurons. Gr64f-Gal4 flies were obtained from J.R. Carlson[34]; UAS-ChR2 flies, from W.D. Tracey Jr.[33]; and pBDP-Gal4, from G.M. Rubin[48]. Control flies for adult fly experiments were obtained by crossing Chrimson virgin female flies to wild-type Berlin (WTB) flies. VT031497-Gal4 flies were from B. Dickson[37].

Larval NMJ experiments. *Fly handling and preparation.* Flies were raised on standard cornmeal-based medium with 0.2 mM all-*trans*-retinal at 25 °C. Wandering 3rd instar larvae were dissected in HL3.1 physiological saline containing (in mM) 70 NaCl, 5 KCl, 0.4 $CaCl_2$, 4 $MgCl_2$, 10 $NaHCO_3$, 5 trehalose, 115 sucrose, 5 HEPES, pH 7.15. Animals were filleted as described previously[31], and the central nervous system was removed. Larval fillets were then mounted on a standard intracellular electrophysiology rig. Temperature was maintained at ~22 °C.

Intracellular recording and stimulation parameters. We used 10- to 15-MΩ sharp intracellular electrodes filled with 3M KCl to record light evoked excitatory junctional potentials in larval muscle 6 (m6). The electrode was maneuvered using an MP-285 micromanipulator (Sutter Instruments). Recordings were amplified with an Axopatch 200B (Molecular Devices) and collected using a Powerlab 16/30 and Chart 7.1 software (both from AD Instruments). We delivered light pulses of either 1, 2, 4, 8, and 16 ms at 470 nm (0.14 mW/mm^2) and 617 nm (0.06 mW/mm^2) or 10, 20, 40, 80, and 160 ms at 720 nm (1 mW/mm^2). Light pulses were generated with LED light sources (470 nm, 617 nm: OptoLED, Cairn Instruments; 720 nm: Thorlabs LED controller), triggered by the Powerlab 16/30 data acquisition system. For each genotype tested, we recorded from two muscles in each of three separate animals. Electrophysiological data were analyzed with custom scripts in Spike2 (Cambridge Electronic Designs).

Adult fly experiments. *Fly handling.* Flies were raised from the egg stage[49] on standard cornmeal and soybean–based medium with 0.2 mM all-*trans*-retinal. Vials were wrapped in aluminum foil to protect retinal from light and kept in a 23 °C, 60% humidity incubator. Flies were transferred to fresh retinal food vials on the first day of eclosion. We used 2- to 3-d-old female flies in PER characterization experiments for 470 nm and 617 nm, and we used 4- to 5-d-old female flies for 720 nm. All flies used to measure behavioral artifacts and the corresponding PER were crossed on the same day, raised side by side in two vials of the same batch of medium and collected on the same day.

Setup for behavioral experiments. The fly preparation and LED display have been published elsewhere[50]. Briefly, female flies were cold anesthetized and placed in a sarcophagus under

a dissection microscope. Then they were tethered with a wire placed between the head and the thorax with UV-activated glue. They were centered in a modular display system[50] (IO Rodeo), which consists of five rows and seven columns of 8 × 8 LED panels (Bright LED Electronics Corp., BM-10B88MD) covering the upper visual field from −105° to +105°. The LED emission surface was covered with a layer of conductive film to minimize electrical noise (Clear Shield, Transparent Conductive Film), two layers of bandpass filter gel (ROSCO, Roscolux #59 indigo), another layer of conductive film, and a layer of stencil paper to prevent reflection. Behavior was recorded using a camera (camera: PointGrey, FFMV-03M2M, lens: Computar, MLM3x-MP, software: Matlab Image Acquisition Toolbox, MathWorks) with an IR illumination source (Oslon, SFH4715S), longpassed at 850 nm (Thorlabs, FGL850) to prevent Chrimson activation. The same filter was used in front of the imaging camera to prevent image corruption from LEDs used for Chrimson activation. We used three high-power LEDs for Chrimson activation (Thorlabs, M470L2, M617L2, and M735L3, respectively) after collimation (Thorlabs, ACL2520-DG6-A for 470 nm and 617 nm, ACL2520-DG6-B for 735 nm, and additional bandpass filtering for 735 nm: Semrock, FF01-720/12-25). Light intensity was measured at the position of the fly (Thorlabs, S130C). The intensity of the random dot pattern was 40 nW/mm^2, and that of IR illumination was 240 μW/mm^2. The overall configuration is shown in **Supplementary Video 1**. PERs to 470-nm and 617-nm light sources by control flies are shown in **Supplementary Figure 15**.

Design and analysis of PER experiments. Pulse width (ms) and LED light intensity (mW/mm^2) were varied in PER experiments. The number of pulses (25) and the frequency (40 Hz) were fixed. For each fly, a total of ten parameter sets (five per parameter) were tested in each lighting condition with five repetitions. The interstimulus interval (ISI) was 30 s. To minimize desensitization, we ordered trials from low to higher light intensity and low to higher pulse widths. The LED was controlled using a data acquisition device (Measurement Computing, USB-1208FS) and the Data Acquisition Toolbox (MathWorks). Fly behavior was recorded using a camera from 1 s before to 2 s after the initiation of each trial. The positions of the neck connectives and the root of the antennae were manually determined. The position of the tip of the proboscis was determined by finding the maximum horizontal coordinate of nonzero pixels after the image was thresholded. The PER score was scaled by the size of the head capsule (**Supplementary Fig. 15a**). All trials were manually proofread to correct image corruption by leg movement. Five flies were used for each combination of wavelength and fly group.

Measurement of light-induced behavioral artifacts. The setup used to measure light-induced behavioral artifacts was similar to that used for PER characterization with the following exceptions: nine Chrimson flies (Gr64f × Chrimson) and nine control flies (WTB × Chrimson) were tested for all conditions in a single day. Flies were given 3 h to settle after tethering. For each wavelength, we used the minimum LED intensity that reliably evoked a PER (**Fig. 3f**). We manually triggered each trial only when flies stopped moving (minimum ISI: 6.5 s). Flow speed for the blue random dot pattern presented on the LED display was 20 pixels/s. For the dark condition, the LED arena was removed from the setup. The startle score was manually assessed by counting the number of legs moving within 2 s of initiation of each trial (scores thus ranged from 0 to 6 with flight assigned a score of 7). Trials were discarded if flies moved before stimulation. No pair of dark and lit arena conditions showed significant difference (paired *t*-test or Wilcoxon signed rank test after Jarque-Bera normality test; *P* level 0.05) except the 720-nm condition for WTB × Chrimson (Wilcoxon signed rank test; $P = 0.004$). For testing differences between the random dot condition at 720 nm and all other conditions (WTB × Chrimson), data in all six conditions were randomly reassigned into each condition to obtain a null distribution of differences between the conditions (10,000 repetitions). No sample showed greater difference than the original one (thus $P < 1/10{,}000$). Matlab and the Statistics Toolbox (MathWorks) were used for all analyses.

Optogenetics of freely behaving intact flies. An LED array (array of Luxeon Rebel, 700 mA, 617 nm, Philips LXM2-PH01-0070) and its driver circuit were custom designed to independently illuminate each quadrant of a circular light arena from the bottom and were controlled by a microcontroller (Arduino) using custom software (see **Supplementary Fig. 16a** for schematic of setup). A diffuser (Optically Colored Cast Acrylic Sheet, 1/8-inch thick, 12 inch × 12 inch, white, McMaster 8505K11) was placed on top of an LED array to produce a homogeneous light field under a white opaque plastic panel with a circular hole, which served as the behavior arena (3D printed, Vero White, Objet Connex 350; hole dimensions: 100-mm diameter, 3-mm depth). The arena was covered by a transparent plastic panel (optically clear cast acrylic sheet, 1/8-inch thick, 12 inch × 12 inch, McMaster 8560K239) to allow video recording. For fly movement imaging, the whole arena was illuminated from above by an IR light source (850 nm), and a thin IR absorption film (Laser-gard PVC film, YAG, Edmund Optics 53-738) was placed between the arena and the diffuser to prevent IR reflection. In a single session (see **Supplementary Video 6**), we illuminated two opposing quadrants of the arena with the LED array for 30 s (0.015mW/mm^2) and switched to the other two quadrants for the next 30 s. The switching protocol was repeated three times for a total video recording of 120 s. For each session (a total of nine sessions were performed for each genotype), we put ~10–20 flies (~2- to 5-d-old males and females) in the arena. The behavior was recorded using a USB3 camera (Flea3, PointGrey, with longpass filter of 800 nm) and custom software. Image analysis was done in Matlab. The background image (an average image over all frames) was subtracted from each frame. Next, any pixels with less than 20% of the maximum pixel value of the frame were set to 0 and others to 1. This generates a white IR-reflected body image of flies with black background. This image was divided into four quadrants. The percentage of flies in quadrants 1 (northeast) and 3 (southwest) was approximated by the percentage of white pixels in those quadrants relative to the total number of white pixels. Finally, we picked a snapshot of each light condition just before switching (at 60 s and 90 s) and performed a paired *t*-test after Jarque-Bera normality test (VT031497-Gal4 × UAS-Chrimson attP18: degrees of freedom (df) = 8, $P = 0.007$; WTB × UAS-Chrimson attP18: df = 8, $P = 0.502$).

41. Jiang, M. & Chen, G. High Ca^{2+}-phosphate transfection efficiency in low-density neuronal cultures. *Nat. Protoc.* **1**, 695–700 (2006).

doi:10.1038/nmeth.2836

42. Stockklausner, C. & Klocker, N. Surface expression of inward rectifier potassium channels is controlled by selective Golgi export. *J. Biol. Chem.* **278**, 17000–17005 (2003).
43. Stockklausner, C., Ludwig, J., Ruppersberg, J.P. & Klocker, N. A sequence motif responsible for ER export and surface expression of Kir2.0 inward rectifier K^+ channels. *FEBS Lett.* **493**, 129–133 (2001).
44. Gradinaru, V., Thompson, K.R. & Deisseroth, K. eNpHR: a Natronomonas halorhodopsin enhanced for optogenetic applications. *Brain Cell Biol.* **36**, 129–139 (2008).
45. Ma, D. *et al.* Role of ER export signals in controlling surface potassium channel numbers. *Science* **291**, 316–319 (2001).
46. Pfeiffer, B.D. *et al.* Refinement of tools for targeted gene expression in *Drosophila*. *Genetics* **186**, 735–755 (2010).
47. Mahr, A. & Aberle, H. The expression pattern of the *Drosophila* vesicular glutamate transporter: a marker protein for motoneurons and glutamatergic centers in the brain. *Gene Expr. Patterns* **6**, 299–309 (2006).
48. Pfeiffer, B.D. *et al.* Tools for neuroanatomy and neurogenetics in *Drosophila*. *Proc. Natl. Acad. Sci. USA* **105**, 9715–9720 (2008).
49. Guo, A. *et al.* Conditioned visual flight orientation in *Drosophila*: dependence on age, practice, and diet. *Learn. Mem.* **3**, 49–59 (1996).
50. Reiser, M.B. & Dickinson, M.H. A modular display system for insect behavioral neuroscience. *J. Neurosci. Methods* **167**, 127–139 (2008).